Laser Physics, Vol. 11, No. 1, 2001, pp. 68–76.

Spectroscopy of the Gases Interacting with Intense Femtosecond Laser Pulses

A. Talebpour*, M. Abdel-Fattah*, A. D. Bandrauk, and S. L. Chin***

** Centre d'Optique, Photonique et Laser (COPL) and Dept. de Physique, Université Laval, Québec, Qc, G1K 7P4 Canada*
*** Laboratoire de Chimie théorique, Faculté des Sciences, Université de Sherbrooke, Sherbrooke, Qc, J1K 2R1 Canada*

e-mail: slchin@phy.ulaval.ca

Received July 21, 2000

Abstract—As a result of focusing ultrafast Ti : Sapphire laser pulses in a gas, a plasma column is created. The spectrum of the radiation from the excited species in the column might be used as a new spectroscopic source free of plasma continuum. Furthermore, from the photoemission spectra, valuable information on the mechanism of interaction of strong laser pulses with atoms and molecules could be obtained.

1. INTRODUCTION

In recent years, the physics of the interaction of atoms and molecules with femtosecond strong laser pulses has been studied extensively. In all the experimental studies the ion and electron signals have been used to probe the mechanisms involved in the phenomenon. These signals, though useful in their own right, are not sufficient to provide all the information necessary for a complete description of the phenomenon. For example, detection of excited neutral molecules and characterization of excited molecular ions is very difficult using ion or electron signal. In these cases the photons emitted by the excited species might be used as a complementary tool. However, to our knowledge, there has been only few reports on utilizing photoemission to probe the interaction of the strong laser field with molecules [1, 2].

Our goal in the present article is twofold. Firstly we will show that the plasma column created as a result of interaction of short laser pulses with molecules can be used as a clean spectroscopic source, especially when a gas with high pressure is under study. When using long pulses, the role of the laser is to generate some seed electrons by multiphoton/tunnel ionization (MPI) and to accelerate them by inverse Bremsstrahlung to collide with the gas molecules and generate new electrons through collisions. Avalanche or cascade ionization follows. Once the density of the electrons reached a critical value breakdown occurs, and a high density plasma is created which has no memory of the laser pulse. On the other hand the mechanism of plasma generation in the interaction of an ultrafast laser pulse is free from the collisions due to the fact the duration of the pulse is short compared to average collision times. The electrons are exclusively created through the MPI in the leading edge of the pulse. As time passes, the increase in the intensity of the pulse cannot lead to an appreciable increase in the density of the electrons, since the defocusing effects caused by the plasma and by the high order nonlinearities decrease the local intensity and thus stops the generation of more electrons [3]. Therefore, once the pulse passed, any point in the focal region will be left with luminous excited species immersed in a low density plasma, with very well defined boundaries. These species radiate to a particularly continuumless spectrum, examples of which will be given in the present article and will be compared with the spectra obtained using long laser pulses.

As a second goal of this article the usefulness of photon signals in studying the mechanism of the interaction of molecules with strong laser pulses will be mentioned. We will choose N_2 molecules for example. The merit of this choice is threefold: (1) the N_2^+ molecular ion in the excited state is very stable and does not fragment easily; (2) the knowledge of the interaction of N_2 with strong laser pulses is useful in modeling the propagation of the laser pulses in the atmosphere, which has recently attracted a lot of attention [3, 4]; (3) there is an extensive literature on the band spectra of the molecule [5].

2. EXPERIMENTAL RESULTS

Our laser system consists of a Ti:Sapphire oscillator followed by a regenerative and two multipass Ti:Sapphire amplifiers that can deliver pulses with energies of up to 100 mJ. The duration of the pulses is 0.2 ns and after compression by a grating compressor the duration is decreased to 200 fs (FWHM). The central wavelength λ is 800 nm. Occasionally we use an Nd:YAG pulsed laser with a duration of 5 ns, λ = 532 nm and maximum pulse energy of 800 mJ. The laser beam is focused using a 100 cm focal length lens into a chamber containing different gases with a variable pressure of 1–700 Torr. The radiation emitted from the plasma is imaged onto the entrance slit of a single shot spectrometer armed with a CCD camera, with a spectral resolution of ~3 Å. When using long pulses the plasma is created in a small near spherical zone in the focal region and from one shot to another the position

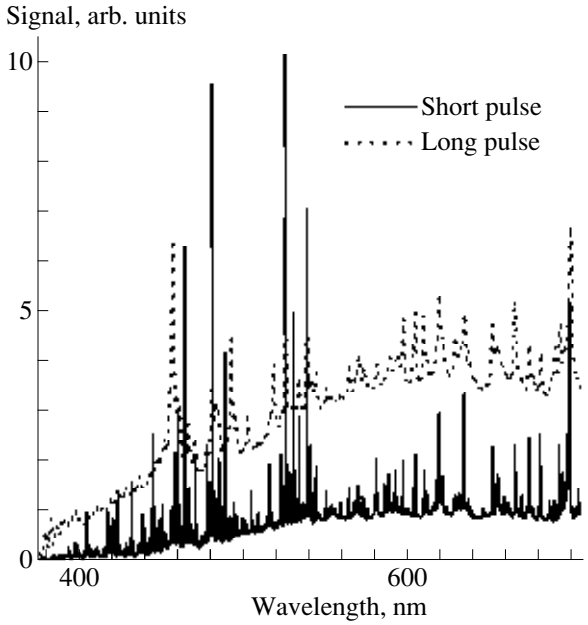

Fig. 1. Spectrum of Xe at a pressure of 10 Torr using long pulses (5 ns, Nd:YAG laser) with an energy of 100 mJ/pulse and short pulse (200 fs, Ti:Sapphire laser) with an energy of 40 mJ/pulse.

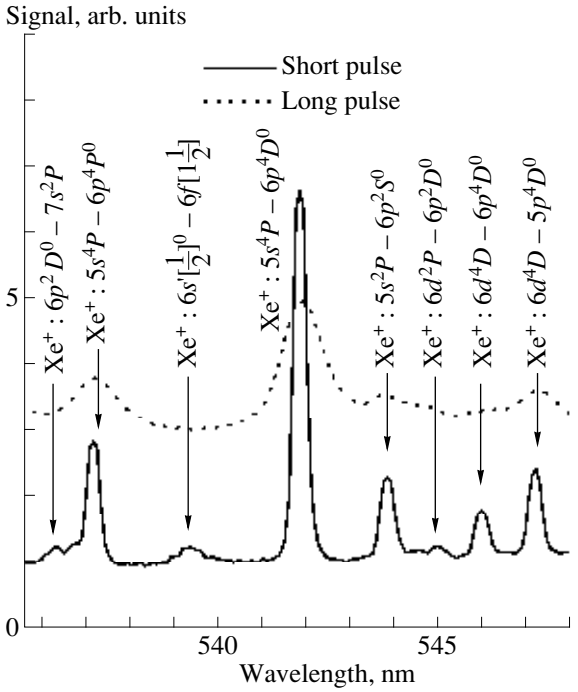

Fig. 2. A narrow portion of Fig. 1, which presents the strong line broadening in the case of long pulses. The identification of the lines is from [6].

of breakdown varies along the propagation axis. The emission spectrum of this breakdown consists of a continuum modulated by the line emissions from atoms and atomic ions. When using the 200 fs laser pulses, spanning around the focal region, a faint filament with a length of about 10 cm is visually observed. The spatial shape of the filament is stable from shot to shot.

In Fig. 1 we present the visible spectrum of Xe with a pressure of 10 Torr interacting with Ng:YAG laser pulses with a duration of 5 ns (dotted line) and compare it with the case of 200 fs Ti:Sapphire laser pulses (solid line). As it is observed there are two distinct differences between the two cases. The first difference is the smaller contribution of the continuum in the case of short laser pulses. In fact, we have noticed that the contribution of the continuum from all other target gases is very small as it will be seen later. This indicates the negligible role of plasma recombination in the process of the photoemission from the plasma column (filament) generated using short laser pulses. The second difference is the amount of broadening in the spectral lines. To show this point, in Fig. 2 we present a limited portion of Fig. 1 in the wavelength interval of 535–548 nm. While the line broadening in the case of long pulses is very strong, the line widths in the case of short pulses, are limited by the resolution of the spectrometer.

The experimental results on Xe showed the merits of using short pulses as being the reduction in continuum radiation and reduced line broadening. We verified this observation by repeating the experiment on different gases. As an example in the case of molecules, in Figs. 3 and 4 we present the spectrum of air in atmospheric pressure in the visible region using long (200 ps) and short (200 fs) Ti:Sapphire laser pulses, respectively. As it is observed, in the case of long laser pulses the emission spectrum of this breakdown consists of two parts; a continuum corresponding to a temperature of about 40000 K modulated by the line emissions from atoms and atomic ions. When short pulses are used there is no detectable continuum radiation in the spectrum, indicating the negligible role of plasma recombination in the process of the photoemission from the filament. This spectrum is assigned to two band systems; the second positive band system of N_2 ($C^3\Pi_u$–$B^3\Pi_g$ transition) and the first negative band system of N_2^+ ($B^2\Sigma_u^+$–$X^2\Sigma_g^+$ transition) [5]. We have indicated the lines of the second positive band and the first negative band with 2 and 1, respectively. We will discuss the origin of this spectrum later in this article. As a final example in Fig. 5 we present the spectrum of ethylene at atmospheric pressure interacting with Ti:Sapphire laser pulses. Again the contribution of the continuum is negligibly small and due to the negligible line broadening rotational structures of the bands are very well resolved.

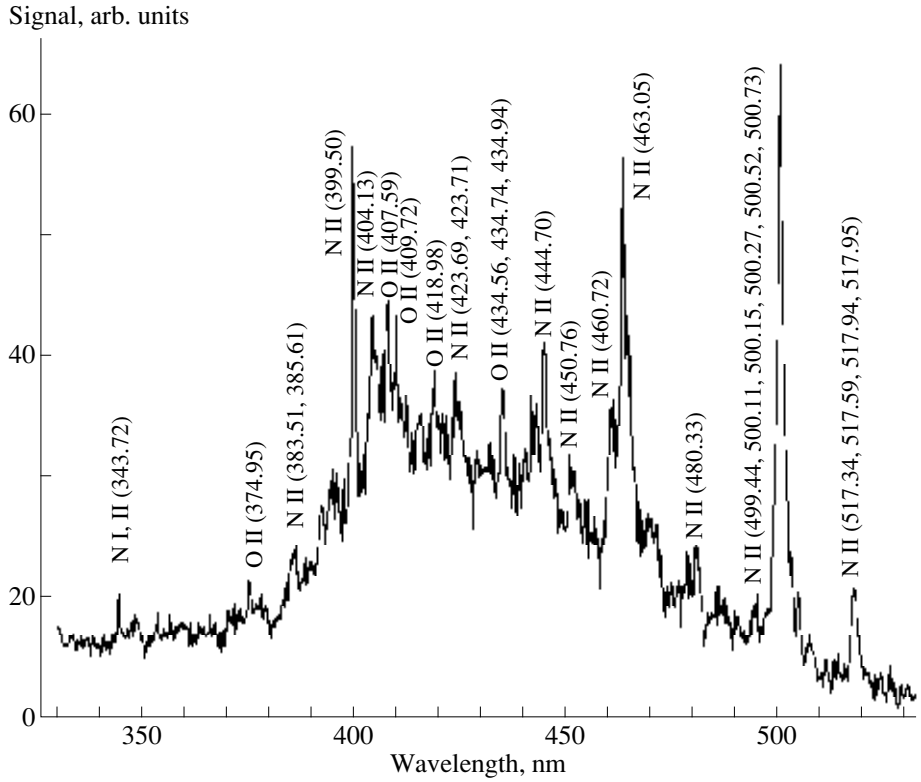

Fig. 3. The emission spectra of air in atmospheric pressure interacting with a Ti:Sapphire laser pulse of duration of 0.2 ns. The identification of the lines is from [6].

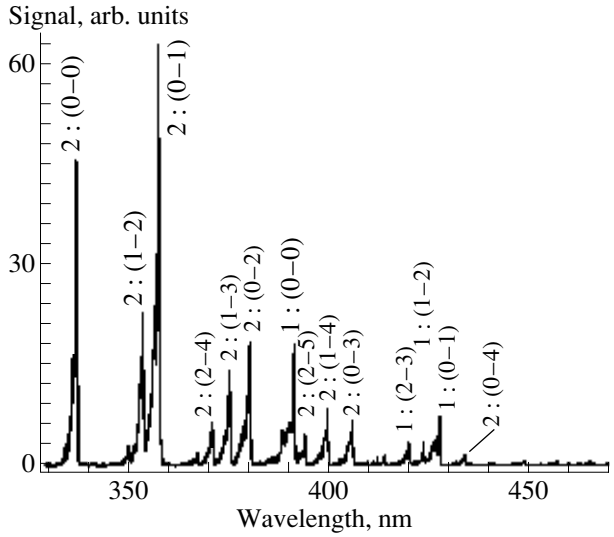

Fig. 4. The emission spectra of air in atmospheric pressure interacting with a Ti:Sapphire laser pulse of duration of 200 fs. The lines marked by 1 are assigned to the first negative band system of N_2^+ ($B^2\Sigma_u^+ - X^2\Sigma_g^+$ transition) and those marked by 2 are assigned to the second positive band system of N_2 ($C^3\Pi_u - B^3\Pi_g$ transition) respectively. In the transitions ($v - v'$), v and v' denote the vibrational levels of upper and lower electronic states, respectively.

3. DISCUSSION

3.1. Negligible Contribution of Continuum Radiation

As it was mentioned in the introduction, the main reason behind the superiority of the spectra in the case of short laser pulses is due to low plasma density. To verify this statement we measure the upper limit of plasma density created in D_2 interacting with 200 fs Ti:Sapphire laser pulses. The merits of this choice are the following. Firstly, during the interaction of D_2 with the laser there is a channel which dissociates the molecule into excited atomic ion, D* [2]. The excited ion fluoresces and the bandwidth of the fluorescence can be used to characterize the plasma density. Secondly, since the Stark broadening in hydrogen depends linearly on the external electric field, the fluorescence lines of H (D) have the largest broadening. This allows the measurement of small plasma densities [7].

First we try to calculate the probability of MPI (here tunnel ionization is included in the definition of MPI) of D_2 as a function of pulse energy under the condition of low pressure. In this case, the effects of self focusing by the neutrals and defocusing due to the plasma is negligible and therefore the intensity of the laser can be calculated easily. For our experiments we use 200 fs Ti:Sapphire laser pulses. The linearly polarized laser was focused using a lens with $f/100$ optics (1 m focal

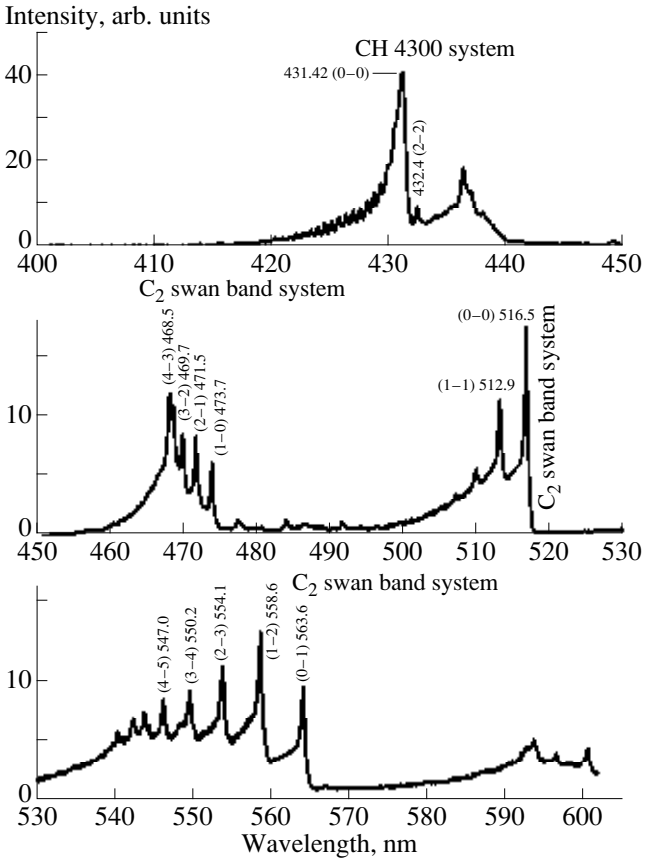

Fig. 5. The emission spectra of ethylene in atmospheric pressure interacting with a Ti:Sapphire laser pulse of duration of 200 fs.

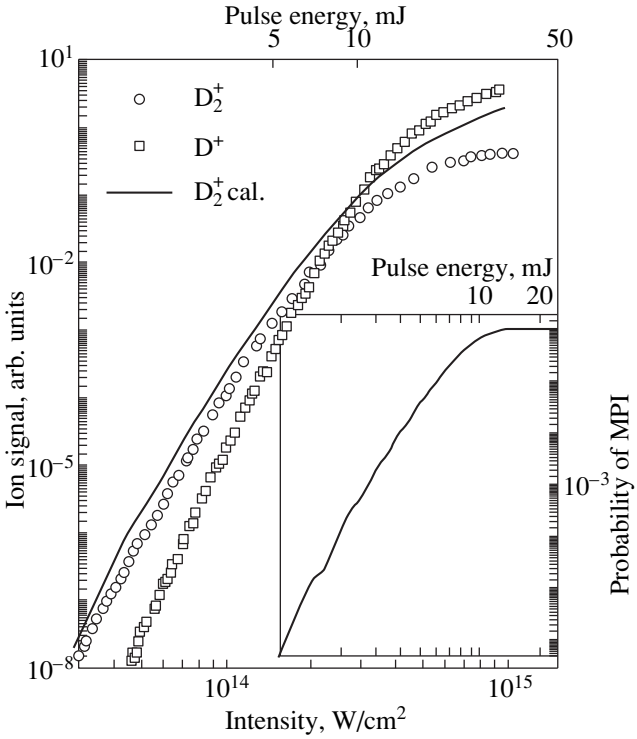

Fig. 6. The ion yield versus peak laser intensity (and pulse energy) curves of D_2^+ and D^+ created as a result of interaction of D_2 with a linearly polarized laser pulse. The theoretical ion signal versus peak laser intensity curve of D_2^+, calculated from the PPT model (see text), has excellent fit with the experimental curve. Also the probability of MPI as a function of peak laser intensity (pulse energy) is shown.

length lens and beam diameter of 1 cm) into an ultrahigh vacuum chamber having a background pressure of 2×10^{-9} Torr. Ion curves were produced by combining a series of intensity scans, each having a different fill pressure in the interaction chamber. The gas pressure in the interaction chamber was controlled by a precision leak valve and ranged from 10^{-8} to 10^{-4} Torr. In Fig. 6 the ion versus pulse energy (upper scale) is presented. In this figure, the horizontal axis (bottom) is in terms of the peak intensity of the laser. The method for determining peak laser intensity is given elsewhere [8].

We note that the ion signal, N_i, is related to the probability of MPI, P_i, through the following relation:

$$N_i = \int_V P_i(\mathbf{r}) dV, \tag{1}$$

where V is that part of the interaction volume from where the ions are collected. To find P_i one should solve this integral equation. However, this is impossible due to the fact that in the experiment we measure only the relative value of the ions. Thus, we chose another approach, i.e., we calculate P_i from the theory in such a way that when it is substituted in Eq. (1), the theoretically calculated curve fit the experimentally measured one. Previously [9], we have shown that the rate of MPI of D_2, W, is very well predicted by the PPT model [10] by assuming that the electron tunnels through a barrier given by $Z_{\text{eff}}/r - Fr$ instead of the pure Coulomb barrier $1/r - Fr$ which is used in the calculation of the MPI of atoms. Here, Z_{eff} (=0.72 for D_2 molecule) is a fitting parameter to simulate the effective Coulomb potential felt by the electron that tunnels out and F is the electric field of the laser. According to this model W is given by the following formula (in atomic units):

$$W = |C_{n^*l^*}| E \sqrt{\frac{6}{\pi}} \left(\frac{2(2E_{nv})^{3/2}}{F} \right)^{2n^* - 3/2} \times (1 + \gamma^2)^{3/4} A(\omega, \gamma) e^{-\left(\frac{2(2E)^{3/2}}{2F} g(\gamma) \right)}, \tag{2}$$

where E is the ionization potential of the molecule, ω is the frequency of the laser and

$$n^* = \sqrt{2E}/Z_{\text{eff}}^2. \tag{3}$$

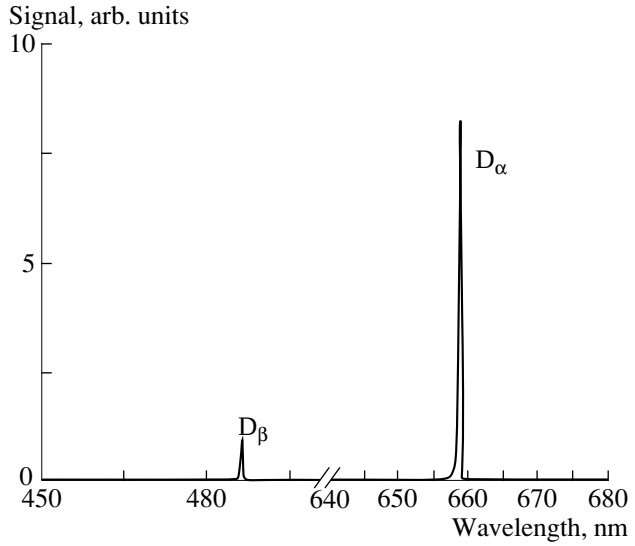

Fig. 7. The emission spectra of D_2, with a pressure of 400 Torr, interacting with a 200 fs Ti:Sapphire laser pulse with an energy of 40 mJ.

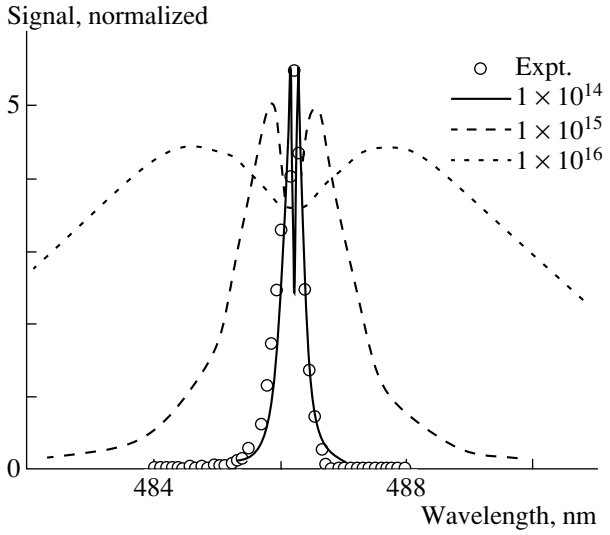

Fig. 8. Comparison of the profile of the D_β line with theoretically calculated profiles at different plasma densities. The densities are in the unit of cm^{-3}.

Other quantities are given in [11]. The probability of the MPI is given by

$$P_i = \left(1 - \exp\left(-\int_{-\infty}^{+\infty} dt W\right)\right). \quad (4)$$

Using this equation we calculated P_i as a function of laser intensity and pulse energy and presented it in the inset of Fig. 6. To see the accuracy of our semi-empirical model, we substituted the calculated value of P_i in Eq. (1) and presented the resulted ion curve in the Fig. 6 (solid curve). As it is observed there is a good overlap between theory and experiment (note that at intensities above 2×10^{14} W/cm^2, corresponding to 13.35 mJ, the dissociation reduces the number of D_2^+ ions to two D^+ ions). Thus we might have confidence on the theoretically calculated value of the probability of ionization plotted in the inset of Fig. 6. From this curve it is observed that under the condition of low pressure, any pulse with energy above 13.35 mJ will ionize all molecules. In what follows we will show that this is not the case for high-pressure gas.

In Fig. 7, we present the spectrum of D_2 at a pressure of 400 Torr. Similar to the case of air, there is no detectable continuum radiation in the spectrum. There are two line emission from D atoms, D_α and D_β. The mechanism of creating excited atoms which radiate these lines is described in [2]. The importance of atomic emission to characterize the plasma created in the interaction region, is well known. Due to the linear Stark effect which occurs in the excited atoms in the presence of plasma, there will be a line broadening. In the case of D_β line this broadening is calculated and its relation to the plasma density is found [7]. In Fig. 8 we have presented the experimental profile of the D_β line (open circles) along with the theoretically calculated line profiles at different plasma densities and at a temperature of 10^4 K. This temperature has been chosen because at low intensities of the order of 10^{13} W/cm^2 (the intensities that the pulses are focused in the high pressure gas) the MPI process corresponds to the absorption of the threshold number of photons, just sufficient to overcome the ionization potential. In this case the kinetic energies of the ionized electrons cannot exceed the energy of a single photon, which corresponds to a temperature of $\sim 2 \times 10^4$ K.

As it is observed from Fig. 8, at the value of plasma density around 10^{14} cm^{-3} theory and experiment fit each other very well. This means that the probability of MPI does not reach above 10^{-5} ($10^{14}/10^{19}$). From Fig. 6 (inset), this probability of MPI corresponds to a laser intensity of 5×10^{13} W/cm^2 instead of 10^{15} W/cm^2 which was expected in the vacuum. Thus, in a high-pressure gas the laser is not able to focus to its geometrical focal size, and the peak intensity of the pulse remains so low that the density of electrons never reaches the critical density necessary for the occurrence of breakdown. This explains why in the spectrum of gases radiated from a filament the level of continuum radiation and the line broadening are so low.

3.2. The Mechanism of Excitation in N_2 Interacting with Ti:Sapphire Laser Pulses

Until here we explained the superiority of the plasma column generated as a result of interaction of short laser pulses in a high pressure gas. In this section

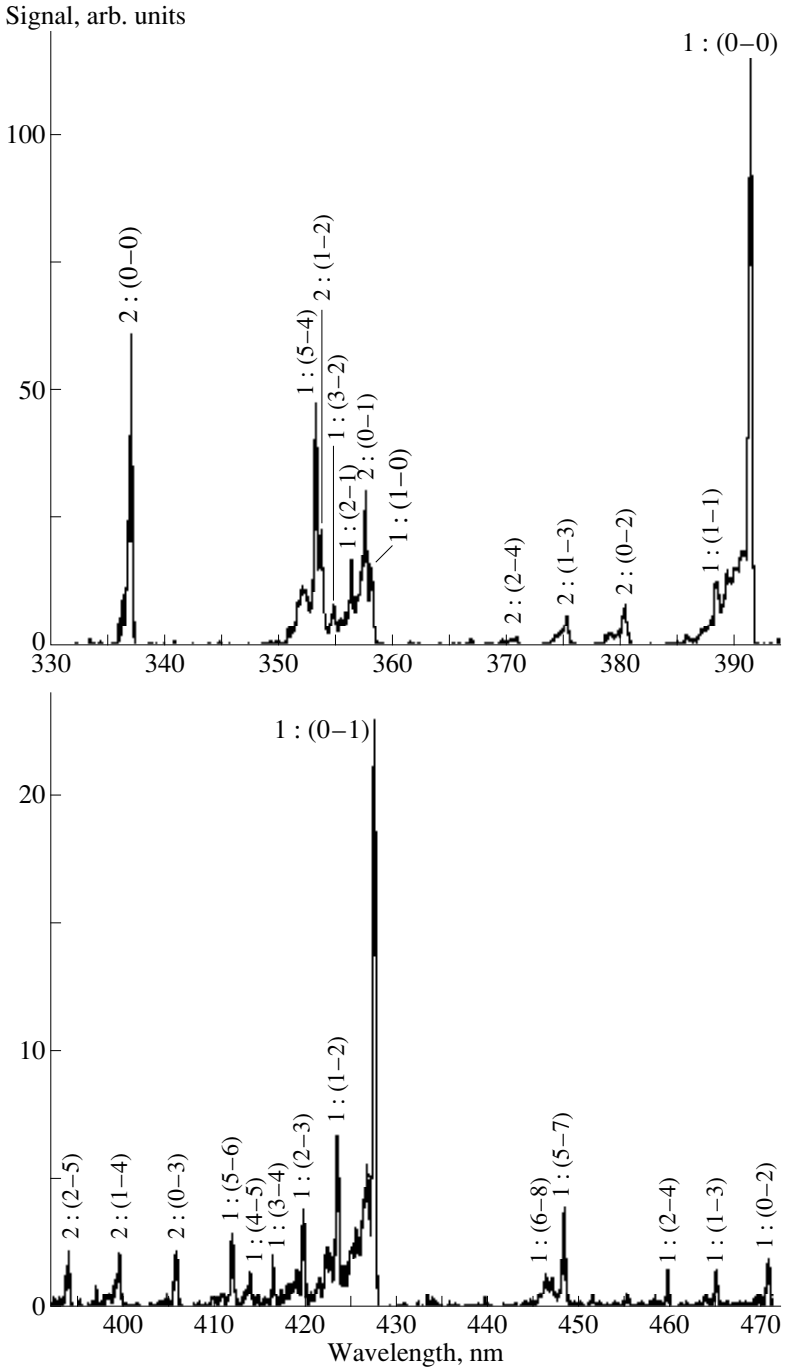

Fig. 9. Spectrum of N_2 at a pressure of 50 Torr interacting with linearly polarized Ti:Sapphire laser pulses at an intensity of 3×10^{14} W/cm^2.

we explain the mechanism of the excitation in the case of N_2. This mechanism, in our opinion, might explain the excitation of species in the case of other gases.

In Fig. 9 we present the resulting calibrated spectrum for the case when the pressure in the tube is 50 Torr. As we mentioned earlier, the observed violet degraded lines are assigned to two systems; the second positive system of N_2 ($C^3\Pi_u$–$B^3\Pi_g$ transition) and the first negative system of N_2^+ ($B^2\Sigma_u^+$–$X^2\Sigma_g^+$ transition) which are labeled in Fig. 9 as 2 and 1, respectively. In the course of this article, it will be made clear that the first negative system is related to inner valence electron ionization. The origin of the second positive band system will only be discussed briefly.

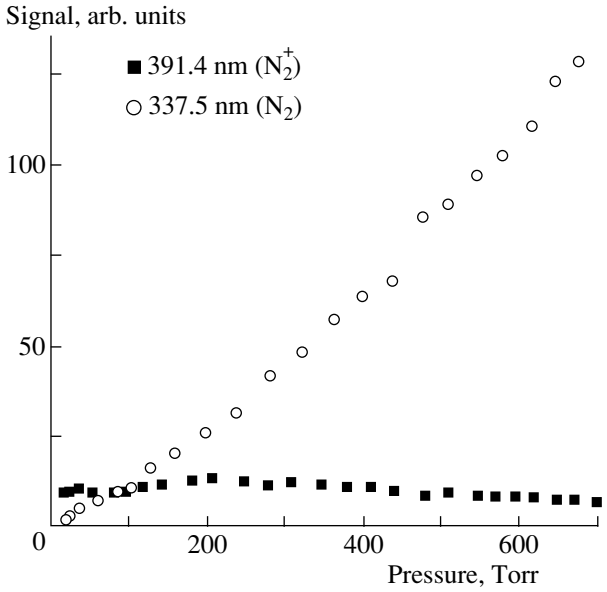

Fig. 10. The pressure dependence of the strength of the two lines 337.13 nm (from the second positive band system of N_2) and 391.4 nm (from the first negative band system of N_2^+) for the case of linear polarization at an intensity of 3×10^{14} W/cm^2.

To probe the excitation mechanism governing these two bands, we have studied the pressure dependence of 391.4 nm band head from the first negative system and the 337.13 nm band head from the second positive band system. From the results shown in Fig. 10 it can be observed that 391.4 nm band head is independent of pressure which could be due to the following reasons. If the excitation mechanism directly results from the interaction of N_2 molecules with the laser pulse, by increasing the pressure the number of molecular ions in the excited state should increase nearly linearly with pressure. At the same time due to collisional deactivation some of the population is transferred from the vibrational levels of the $B^2\Sigma_u^+$ electronic state to the vibrational levels of the $A^2\Pi_u$ electronic state. This process reduces the number of the excited molecular ions, which emit to the first negative band. Since the deactivation process depends linearly on pressure [12], the number of excited ions capable of emitting decreases as the inverse of pressure. Consequently the strength of the band heads of the first negative band should not depend on pressure. In contrast to this, it can be observed from Fig. 10 that the strength of 337.13 nm band head increases linearly with pressure. Extending similar arguments to the case of the bands of the second positive system, the number of excited molecules in the $C^3\Pi_u$ electronic state must depend on the square of pressure. This could imply that the mechanism of populating the vibrational levels of the upper electronic state ($C^3\Pi_u$) might be resulting from a combination of two pressure dependent processes, one being collision and the other being laser excitation whose product also depends linearly on pressure. However, our experimental results cannot determine the dynamics of the laser excitation mechanism.

To obtain further information on the mechanism of the photoemission in the first negative band, we measured the laser intensity dependence of the strength of the 391.4 nm band head using linearly and circularly polarized laser pulses with the pressure set at 1 Torr (Fig. 11). The 391.4 nm band head was chosen because of its higher strength compared to the other band heads. The resulting curves are compared with the ion yield versus laser intensity curves of N_2^+ obtained from an independent experiment in a vacuum chamber and were presented in Fig. 3. For comparison of the measured curves of the ion yield and the strength of 391.4 nm band head, we use the saturation points of the curves indicated by an arrow in Fig. 11. The strength of the band head was shifted vertically in order to bring the two curves to the same level in their respective saturation intensities. There is no horizontal shift. The overlap of the two curves for both polarizations indicates a close relation between the MPI of the neutral molecule and the excitation of the N_2^+ ion to $B^2\Sigma_u^+$ electronic state. The two possible reasons that could explain these observations, are considered below.

As a first possibility, the ionized electron can re-scatter to its parent ion [13] and through an inelastic collision excite the ion to the vibrational levels of higher electronic states. At the intensities employed in our experiment, 3×10^{14} W/cm^2, the ponderomotive energy, U_p, amounts to 18 eV and many of the re-scattered electrons have energy of $3.2U_p$ = 58 eV. These electrons can excite the N_2^+ ions to the $v = 0$ and $v = 1$ vibrational levels (these are the only vibrational levels which have significant Franck–Condon factors for coupling with the $v = 0$ level of the ground electronic state [5]) of the $B^2\Sigma_u^+$ electronic state. However, this possibility can be ruled out by comparing the laser polarization dependence of the strength of those band heads of the first negative system of N_2^+ originating from the $v = 0$ and $v = 1$ vibrational levels of the $B^2\Sigma_u^+$ electronic state. The strength of these band heads has dropped only by a factor of ~5 after changing the polarization from linear to circular as shown in Fig. 11. This can be attributed to the decrease in the probability of MPI as a result of changing the polarization of the laser from linear to circular. The classical picture of electron re-scattering model predicts that the probability of exciting the molecular ion in the case of circular polarization decreases to zero which has not been observed in our experimental results which are shown in Fig. 11.

The other possibility is populating the $B^2\Sigma_u^+$ state through the MPI of inner valence electrons which has been used with great success for the explanation of the observed photoelectron spectra of N_2 molecule interacting with 308 and 616 nm laser pulses [1]. The electronic configuration of N_2 molecule is $KK(\sigma_g 2s)^2(\sigma_u 2s)^2(\pi_u 2p)^4(\sigma_g 2p)^2$. If instead of the two electrons of the outermost orbital ($\sigma_g 2p$), any of the electrons of the inner orbitals ($\pi_u 2p$) or ($\sigma_u 2s$) is ionized through MPI, the resulting molecular ion will be produced in a vibrational level of the excited electronic states $A^2\Pi_u^+$ or $B^2\Sigma_u^+$, respectively. The number of the ions in the excited states $A^2\Pi_u^+$ or $B^2\Sigma_u^+$ will be nearly proportional to the total number of ions. Therefore the strength of the band heads of the first negative band system will have a similar intensity dependence as the number of ions. This conclusion is in agreement with the observation in Fig. 11. In particular by changing the polarization of the laser the number of ions and the strength of the band head decrease at the same rate. Thus, this model is able to explain the origin of excitation to the $v = 0$ and $v = 1$ levels of the $B^2\Sigma_u^+$ electronic state which results in emission to two of the strongest band heads of the first negative system at 391.44 nm [(0–0) transition] and 427.81 nm [(0–1) transition].

However, this model cannot explain the appreciable emission from those vibrational levels of $B^2\Sigma_u^+$ electronic states with $v \geq 2$, since the MPI of the electrons of the $\sigma_u 2s$ orbital cannot populate these higher vibrational levels due to the small Franck–Condon factors [5]. To account for the population of those levels of $B^2\Sigma_u^+$ with $v \geq 2$ we might consider the mechanism of up-pumping of population from those levels of the $X^2\Sigma_g^+$ and $A^2\Pi_u^+$ electronic states which are appreciably populated during the MPI of N_2. The up-pumping is accomplished either by three photon coupling from the $v = 0$ level of $X^2\Sigma_g^+$ electronic state (similar to the three photon coupling as in the case of H_2^+ discussed in [14, 15]) or by a two photon coupling from the $v = 0$ and $v = 1$ levels of $A^2\Pi_u^+$. In the former case, since a three photon transition is in quasi resonance with the $v = 5$ level of the $B^2\Sigma_u^+$ state, most probably this level will be populated. In the latter case, a two photon resonance will populate the levels $v = 3$ and $v = 4$ of $B^2\Sigma_u^+$ state. To test the validity of this mechanism the dependence of the strength of the band heads on the polarization of the laser might be used. Since by the selection rules the foretold three photon and the two photon couplings are forbidden, using circular polarization it is expected that in this case the strength of band heads

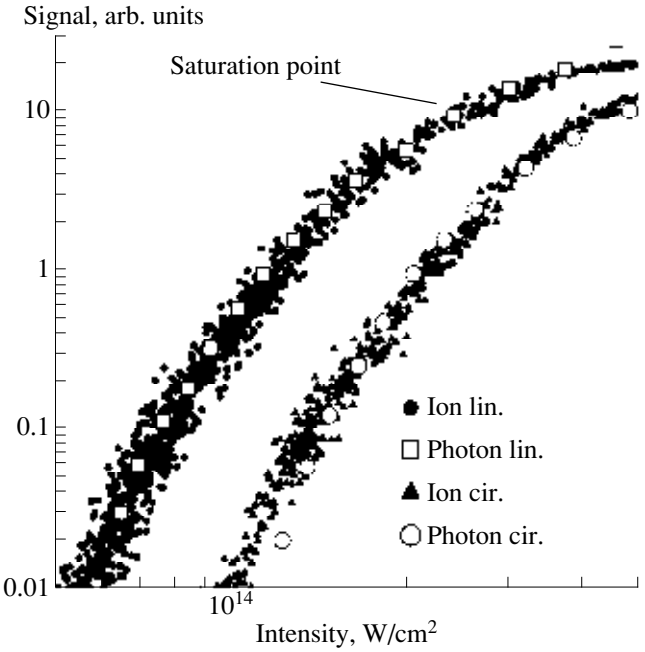

Fig. 11. Comparison of the intensity dependence of the strength of the 391.4 nm band head (open square for linear polarization and open circles for circular polarization) and the number of N_2^+ ions created by pulses with different polarization of laser. The saturation point for the linear polarization is indicated by arrow. The photon signals (the strength of the band head) for both polarizations have been shifted vertically to bring the level of this signal to the same level of their respective ion signals at the saturation point.

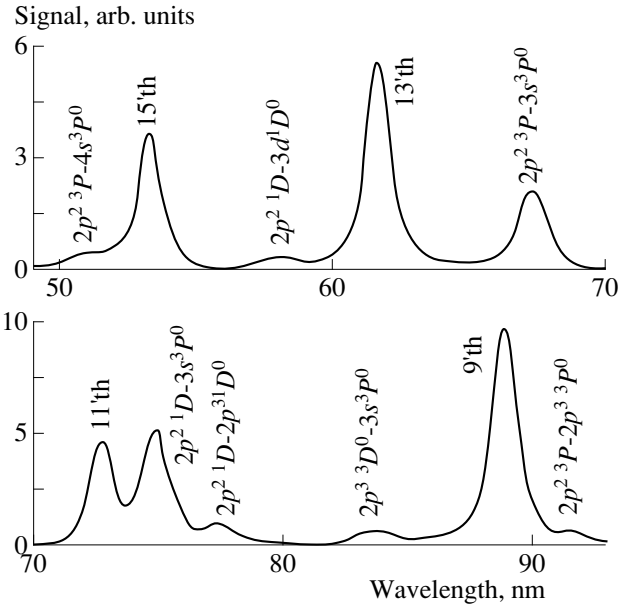

Fig. 12. The UV spectrum of N_2 gas jet interacting with a linearly polarized Ti:Sapphire laser pulse at an intensity of 3×10^{14} W/cm^2. Apart from high order harmonics there are two peaks resulting from the photoemission of N^+. The assignment of the lines are from [6]. Note that each peak usually contains few lines which due to the low spectral resolution of our system have not been resolved.

originating from those levels of $B^2\Sigma_u^+$ with $v \geq 2$ must drop to zero. Indeed, we observed that the signal decreases to zero when circular polarization was used, in agreement with the prediction of the model.

The foregoing arguments strongly suggest the occurrence of MPI of the inner valence electrons in N_2. To reinforce this suggestion, we did a further experiment. The laser was focused into a pulsed N_2 gas jet at a position of about 10 μm under the jet nozzle where the pressure of the gas jet is about 40 Torr. The working pressure of the vacuum chamber is 5×10^{-7} Torr. The radiation in the forward direction is separated by a concave grating which images the lines onto a microchannel plate with a phosphored fiber optic anode. The image on the anode is recorded by a CCD camera and thus the spectrum is obtained [2]. A sample spectrum in the wavelength region $49 < \lambda < 93$ nm is presented in Fig. 12. Apart from high order harmonics there are seven peaks in the spectrum which are radiated by the N^+ ions created as a result of the interaction of the laser pulse with N_2 molecule. The transitions responsible for these peaks are identified in Fig. 12. Similar photoemission has been observed previously in experiments involving the interaction of N_2 molecule with synchrotron radiation [16] and electrons [17]. There, it has been argued that the creation of the excited atomic ions is due to the removal of an inner shell $\sigma_g 2s$ electron which results in a N_2^+ molecule in $G^2\Sigma_g^+$ repulsive electronic state which dissociates to N^+ ions in $^3P^0$ state. Later experimental and theoretical results (see [18] and references therein) verified this statement. The similarity of our observation with this well established finding suggests that in the interaction of N_2 molecule with Ti:Sapphire laser the inner shell electrons undergo MPI.

4. CONCLUSION

In conclusion by comparing the spectra radiated by self-luminous plasmas created by a laser pulse interacting with a gas target we have shown that the spectrum resulting from the interaction of ultrashort pulses is far superior in terms of low level of continuum and also smaller line broadening. This was attributed to the lower density of the plasma in the case of short laser pulses due to the defocusing effects which limits the intensity of the pulse in the interaction region and thus prevents further multiphoton/tunnel ionization of the gas. We verified our statement by measuring the upper limit of the plasma density in D_2. Also the mechanism of excitation was determined in the case of N_2 molecule. Our observations indicate that the first two vibrational levels of the $B^2\Sigma_u^+$ state are populated as a result of the MPI of the inner valence electrons ($\sigma_u 2s$ orbital). In the UV region the photoemission from N^+ ion was observed. The creation of this ion in the excited state was attributed to the MPI of the inner shell electron $\sigma_g 2s$. The phenomenon of the MPI of electrons from the inner orbitals has been confirmed from these observations.

ACKNOWLEDGMENTS

It is our pleasure to acknowledge the technical assistance of S. Lagace and M. Lambert and fruitful discussions with C.M. Bowden and N. Akozbek. This work was supported in part by NSERC, le Fonds FCAR, US Army Research Office and the Department of National Defense of Canada.

REFERENCES

1. Gibson, G. *et al.*, 1989, *Phys. Rev. A*, **40**, 2378.
2. Liang, Y. *et al.*, 1995, *J. Phys. B*, **28**, 3661.
3. Akozbec, N., Bowden, C.M., Talebpour, A., and Chin, S.L., 2000, *Phys. Rev. E*, **61**, 4540.
4. Brodeur, A. *et al.*, 1997, *Opt. Lett.*, **22**, 304; Mlejnek, M., Wright, E.M., and Moloney, J.V., 1998, *Opt. Lett.*, **23**, 182.
5. Lofthus, A. and Krupenie, P.H., 1977, *J. Phys. Chem. Ref. Data*, **6**, 113.
6. Striganov, A.R. and Sventitski, N.S., 1968, *Tables of Spectral Lines of Neutral and Ionized Atoms* (New York: IFI).
7. Griem, H.R., 1964, *Plasma Spectroscopy* (New York: McGraw-Hill).
8. Talebpour, A., Petit, S., and Chin, S.L., 1999, *Opt. Commun.*, **171**, 285.
9. Talebpour, A., Larochelle, S., and Chin, S.L., 1998, *J. Phys. B*, **31**, L49.
10. Perelomov, A.M., Popov, V.S., and Terent'ev, M.V., 1966, *Sov. Phys. JETP*, **23**, 924.
11. Talebpour, A., Yang, J., and Chin, S.L., 1999, *Opt. Commun.*, **163**, 29. There are some printing errors in this paper. In Eq. (2), Z should be read Z_{eff}, Eq. (3) should be $\gamma = \frac{\omega\sqrt{2E_i}}{F}$, and in Eq. (8), W_n should be w_n. The $\times$ sign should not be there.
12. Comes, F.J. and Speier, F., 1971, *Z. Naturforsch.*, **26a**, 1998.
13. Corkum, P.B., 1993, *Phys. Rev. Lett.*, **71**, 1994.
14. Bandrauk, A.D., 1994, *Molecules in Laser Fields* (New York: Marcel Dekker).
15. Chelkowski, S., Foisy, C., and Bandrauk, A.D., 1998, *Phys. Rev. A*, **57**, 1176.
16. Lee, L.C. *et al.*, 1974, *J. Phys. Chem.*, **61**, 3266.
17. Aarts, J.F.M. and De Heer, F.J., 1971, *Physica*, **52**, 45.
18. Baltzer, P. *et al.*, 1992, *Phys. Rev. A*, **46**, 5545.